

Li-Defect Interactions in Electron-Irradiated *n*-Type Silicon[†]

Bernard Goldstein*

RCA Laboratories, Princeton, New Jersey 08540

and

*Groupe de Physique des Solides[‡]**Ecole Normale Supérieure et Faculté des Sciences, Paris, France*

(Received 20 April 1970)

Single-crystal silicon, both with and without oxygen, has been diffused with lithium to concentrations $\sim 10^{17}/\text{cm}^3$, irradiated with 1–1.5-MeV electrons, and the ensuing defects studied by EPR and electrical measurements. The presence of oxygen strongly affects the properties of these defects. In O-containing material, the room-temperature carrier-removal rate is 0.25 cm^{-1} , and the carrier concentration continues to decrease after the cessation of the irradiation; in O-free material, the carrier-removal rate is 0.39 cm^{-1} , but here the carrier concentration can either increase or decrease after cessation of the irradiation. EPR measurements have indicated the presence of two new defects which involve Li – one in O-containing material and one in O-free material. Their introduction rates are much smaller than the carrier-removal rates. The defect in O-containing Si exhibits a strong hyperfine interaction with the Li^7 nucleus, while that in O-free Si exhibits no hyperfine structure. Their g values are 2.0046 and 2.0090, respectively, and are isotropic. The defects are observed in their electron-filled state, and indicate a net electron spin of $\frac{1}{2}$. The defect spectra disappear (with time) at room temperature, and this, together with the carrier-concentration changes, can be explained by the formation of other Li-involved defects which lie deeper in the energy band gap and are not visible by EPR. Electron irradiation at 40 °K followed by annealing at higher temperatures show that both EPR defects described above begin to form at about 200 °K and begin to decrease at about 275 °K – just as does the 250 °K reverse annealing observed generally for *n*-type Si. Based on these data, and the work of others, it is suggested that both defects form as a result of the motion of Si interstitials which produce a (Li-O-interstitial) complex in O-containing Si, and a (Li-interstitial) complex in O-free Si.

I. INTRODUCTION

When silicon is irradiated with electrons having an energy above a certain threshold value,¹ lattice defects are produced. When these defects have sufficient mobility, they are either annihilated by recombination processes and migration through the lattice to surfaces, or they become trapped by, and form complexes with, other defects and impurities. Radiation-damage studies have yielded much information and clarification of the basic properties of such complexes and the way in which they are formed, although the present picture is far from completely clear.²

Recent studies have indicated that the general radiation-damage behavior in *n*-type Czochralski-grown Si, doped with different group-V donor atoms, is quite similar for bombarding electrons having energies of 1–2 MeV. For example, the configuration and symmetries of the defect complexes, their stability at room temperature, their effect on carrier concentration, and their temperature behavior are generally very similar or follow very similar patterns.^{3,4} However, the radiation-damage properties of *n*-type Si doped with lithium seems to be very different.⁵ For example,

defect complexes which involve Li are not stable at room temperature,⁶ and their effects on minority carrier lifetime are different from those when Li is absent.⁷ Recent work on Li-doped Si has presented results of optical⁸ and electrical⁹ measurements. We will present and discuss in this paper some results of electron paramagnetic resonance (EPR)^{10–12} measurements of Li-doped Si after electron irradiation.

Two series of experiments will be described. The first involves resistivity and EPR measurements after electron irradiation at 250 °K only. These have enabled us to study many of the basic properties of the observable paramagnetic defect complexes. The second involves EPR measurements after low-temperature irradiations (starting at 40 °K), followed by annealing to successively higher temperatures. This has enabled us to study the formation and annealing of the defect complexes, and ultimately to suggest their composition and formation mechanisms.

II. EXPERIMENTAL RESULTS

A. Apparatus and Procedures

Two types of single-crystal Si were used: One was grown by the Czochralski method and con-

tained $\sim 5\text{--}10 \times 10^{17}/\text{cm}^3$ oxygen; the other was grown by vacuum float-zone techniques and contained less than $5 \times 10^{13}/\text{cm}^3$ oxygen.¹³ We expected that oxygen might play a role in the radiation-damage behavior because of its pairing with Li and its effect on Li diffusion,¹⁴ and its trapping of primary defects.¹⁵ The starting resistivities of the float-zone (O-free) and the Czochralski (O-containing) material were 2000 and 50 Ω cm, respectively. The Si was crystallographically oriented and cut into bars. Lithium was diffused into the Si either from a 1% -Li-99% -Sn bath, or from evaporated layers at temperatures of 400–525 °C to produce homogeneous concentrations of $1\text{--}2 \times 10^{17}/\text{cm}^3$. For the same diffusion conditions, both the O-free and O-containing material gave the same resistivity (about 0.1 Ω cm), indicating that the O was not producing any measurable concentration of donors. Diffusion from Li-in-oil suspensions¹⁴ did not give reproducible results, and often the resulting resistivity changed with time, suggesting that some precipitation may have been taking place. After diffusion, the material was cleaned and chemically etched¹⁶ to a size of 1.5 \times 0.5 \times 7.0 mm.

The source of electrons was a Van de Graaff accelerator which produced a uniform monoenergetic beam of electrons. The fluences generally covered a range from less than to greater than the Li concentrations. They were measured by a Faraday cup arrangement. After the irradiations, the samples were refrigerated and stored at liquid-nitrogen temperatures until measurements were made. Resistivity measurements were made at room temperature with an iridium-tipped four-point probe apparatus. For *in situ* dynamical measurements of the resistivity during irradiation, a simulated four-point probe was used consisting of four contacts to the Si bar made with a Hg-In-Tl alloy¹⁷ which required no heating and functioned as Ohmic contacts over the temperature range of our experiments.

For the first group of experiments, EPR measurements were made with a Varian spectrometer operating at about 9.1 GHz in the absorption mode. The modulation frequency was 100 kHz with amplitudes of 0.3–0.6 G. The sample bars were held in geometrically reproducible positions within the microwave cavity with the aid of a fitted quartz Dewar. Uniaxial compressional stress up to 140 kg/cm² could be applied by transmission along a Lucite rod to the sample bar which was pocketed by two Teflon cups at the ends of the bar. The application of external stress was introduced into our experiments for two reasons: (a) It removed the ground-state degeneracy of the donor-level system produced by isolated interstitial Li,¹⁸ thus enabling us to observe an identifiable EPR absorp-

tion,¹⁹ and (b) it was thought that it might affect an impurity-defect complex by changing its distribution of orientations from random to preferred ones.²⁰ In the latter case, preferred orientations would be visible from the angular dependence of the EPR spectra. All these EPR measurements were made at liquid-neon temperatures, 27 °K.

For the second series of measurements, a Thompson-Houston spectrometer was used. Its only significant difference from the Varian apparatus was that its modulation frequency was 4.2 kHz. However, a special Dewar arrangement had to be constructed to accommodate *in situ* low-temperature electron irradiations and EPR measurements. This Dewar is shown schematically in Fig. 1. It is essentially a quartz tubular extension attached to a metal cryostat²¹ with indium-gasket vacuum seals. The Si sample is attached to a 2000- Ω -cm Si support rod, which is in turn connected to a metal rod which can be rotated, raised, and lowered. For EPR measurements only the support rod and Si sample enter the microwave cavity. During operation the metal cryostat acts as a liquefier when a pressure of about 1 atm of H₂ is admitted into the central tube. For annealing purposes, the H₂ is removed from the central tube of the cryostat, and the Si sample is heated by an external annular resistance furnace. All EPR measurements in this series were made at liquid-H₂ temperatures, 20 °K. A Chromel-constantan thermocouple recorded the irradiation and annealing temperatures.

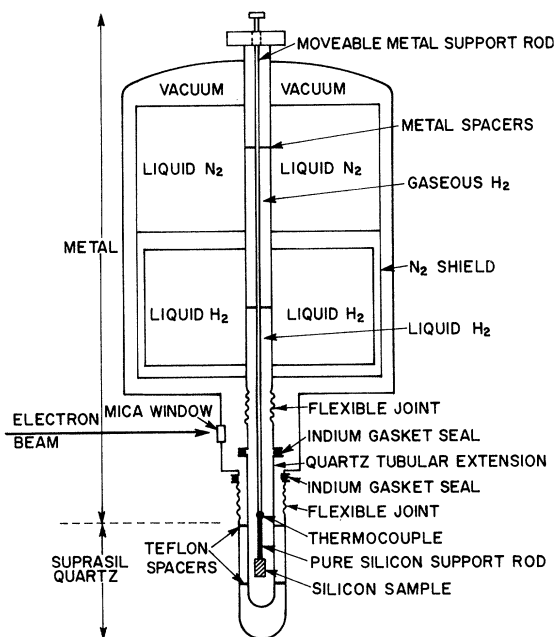


FIG. 1. Schematic representation of metal-quartz cryostat.

B. Resistivity Behavior

Irradiation with 1-MeV electrons produces deep acceptor levels which can act as electron traps and thus reduce the electron carrier concentration. Figure 2 shows the total carrier-removal rates for both O-free and O-containing Si after irradiation at 252 °K. These rates are different, and indicate either that we are forming different defects or we are forming the same defects but at different rates. However, the EPR results to be discussed later indicate that we are dealing, at least in part, with different defect centers. The carrier-removal rates of 0.25 and 0.39 cm^{-1} for O-containing and O-free Si, respectively, are of the same order as those reported for group-V dopant atoms³ at similar energies; in addition, the effect of O is also similar, i. e., the carrier removal rate is invariably higher for float-zone material. In Fig. 3, we show an important difference between electron-irradiated Si doped with Li and other *n*-type dopants. At room temperature, there are spontaneous changes in resistivity with time.²² For O-containing material there is a decrease in charge carriers with time, while for O-free material there is an increase. These are characterized by rapid initial changes, followed by regions of much slower change. As can be seen, the total initial and final decrease in carrier concentration still varies with increased fluence.

Several other samples containing different initial Li concentrations were irradiated and mea-

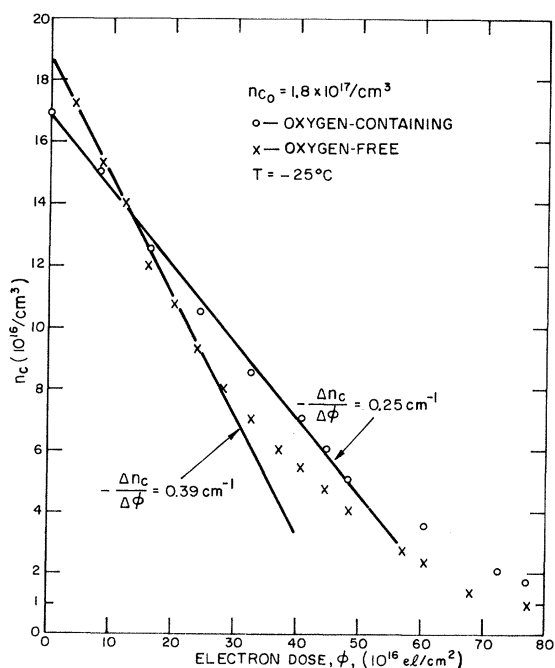


FIG. 2. Changes in carrier concentration during electron irradiation.

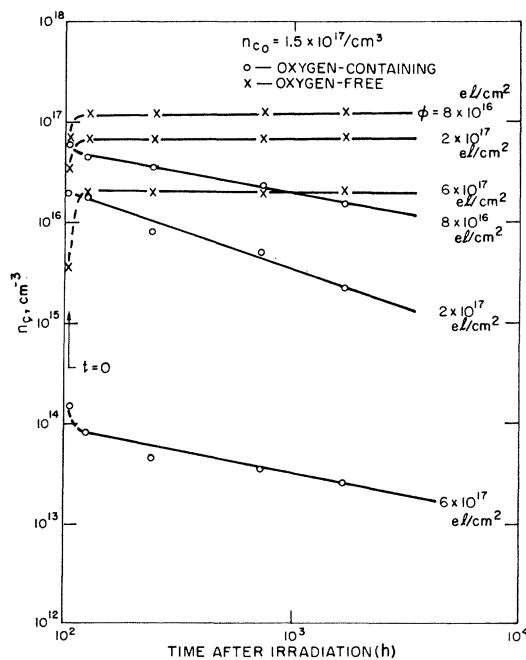


FIG. 3. Changes in carrier concentration with time after cessation of electron irradiation. The fluence ϕ of each irradiation is given at the right of each curve.

sured. In all cases, the O-containing samples showed spontaneous carrier removal at room temperature after irradiation as in Fig. 3. However, some of the O-free samples showed behavior opposite to that shown in Fig. 3, i. e., carrier *decreases* with time (this behavior is discussed in some detail in Sec. III). The decreases in carrier concentration invariably follow a power law, although the exponent varies from sample to sample. In O-free material, the final equilibrium situation is always approached much faster than in O-containing material.

C. Electron Paramagnetic Resonance Measurements

1. Irradiation at 250 °K

The EPR absorption lines we will be dealing with are those of the (Li-O) shallow donor²³ observed in O-containing material, the stress-induced isolated Li shallow donor¹⁹ observed in O-free material, the various (paramagnetic) damage centers, and the conduction electrons. The resonance of the conduction electrons was used for location and calibration purposes. The Li and (Li-O) resonance lines have *g* values which are so close that they cannot be readily resolved with our instrumentation. However, we will see that these lines do not interfere with the damage spectra, all of which were found within 20 G of the donor resonances.

The external stress used to produce the Li

line was applied in a $\langle 110 \rangle$ direction up to 140 kg/cm². This was more than enough to produce a maximum in the intensity of the Li line.²⁴ In addition, we found that application of external stress also increases the magnitude of the (Li-O) line – by amounts of 20–30%. This was observed in many crystals. It is apparently due to the fact that not quite all of the Li has paired with the O, and we are picking up the unpaired Li in the strain sensitivity.

In Fig. 4, we show the EPR spectrum of Li-doped O-containing Si bombarded by 1-MeV electrons, under conditions described in the figure. It consists of a four-line group, a single line due to the (Li-O) donor, and, at the extreme left, one of the doublet lines due to phosphorus – the trace contaminant in this material. Note the location of the conduction electron resonance indicated by the arrow. The appearance of the four-line group, equal separations and equal heights, marks it as a hyperfine quadruplet. As the fluence increases, the magnitude of the quadruplet spectrum increases while that of the (Li-O) donor resonance decreases. The four-line spectrum indicates an interaction with the Li⁷ nuclear spin of $\frac{3}{2}$. There is no atom which has a nuclear spin of $\frac{3}{2}$ in the lattice. The hyperfine splitting of this spectrum is 3.1 G, roughly ten times greater than that reported for the (Li-O) shallow donor.²³ This spectrum appears only in Li-doped Si, and only after electron bombardment. We conclude from these data that this spectrum is

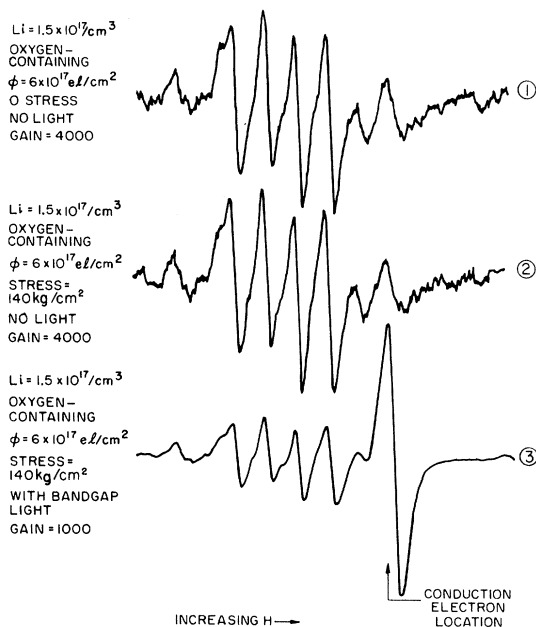


FIG. 4. EPR spectrum of electron-irradiated O-containing Si showing the Li⁷ hyperfine quadruplet and the (Li-O) donor line just to its right.

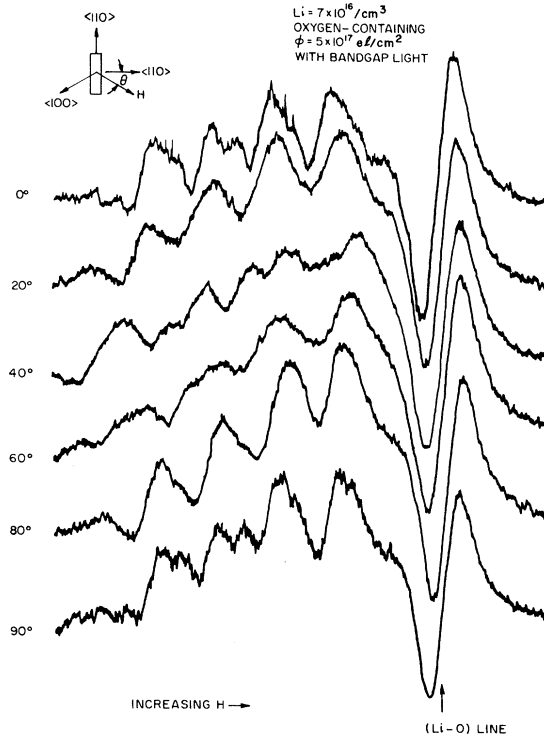


FIG. 5. Angular dependence of EPR spectrum of Fig. 4.

due to a Li-defect complex, with a net electron spin of $\frac{1}{2}$, whose electron is more tightly bound than that of the (Li-O) donor.

Irradiation with band-gap light increases the intensity of the defect resonance and, to a much greater degree, that of the (Li-O) donor resonance. This indicates that since the material was *n* type, and at least some of the shallow donor states remain (unionized) and can be repopulated,²⁵ we are seeing the defect in its filled state. Assuming that the band-gap light has essentially saturated the defect levels, an introduction rate of about 0.02 cm⁻¹ can be measured. When we compare this with the total carrier-removal data in Fig. 2, we can see that only a fraction of the total defects formed are visible by EPR.

The *g* value of the four-line spectrum (at its center) is 2.0046 ± 0.0008 . Its angular dependence is shown in Fig. 5, where with \vec{H} in the (110) plane we can view all primary crystallographic directions. The *g* tensor is isotropic although the hyperfine interaction is not. Note that there is no indication of axial symmetry so frequently observed for defects and complexes in electron-irradiated Si.²⁶ We will return to this point later in the discussion. The hyperfine lines seem best resolved in (or near) the $\langle 110 \rangle$ and $\langle 100 \rangle$ directions. In addition, they appear to be doublets in these directions, and may reflect the distribution of the hyperfine axis among

three equivalent directions; however, the poor signal-to-noise ratio precludes any firm discussion of these data.

The O-free material shows no trace of the four-line spectrum after electron irradiation, suggesting that the Li complex discussed above also involves oxygen. Rather, a single line appears, as shown in Fig. 6. It has a g value of 2.0090 ± 0.0008 , is isotropic, and exhibits no measurable structure. Since it appears only in Li-doped material after irradiation, it too is suggested to be a Li-defect complex. Its introduction rate is $\sim 0.01 \text{ cm}^{-1}$, so that again we are seeing only a fraction of the total number of defects formed. It is only slightly affected by light or strain. External stress reduces its peak magnitude, although it does not change its isotropic character. Normally, one might expect the effects of a varying strain field to change the populations of the shifting energy levels involved in the EPR transitions, and so change the appearance of a group of narrow lines or the shape of a broader line, but such effects were not observable.

As the fluence decreases, the one-line spectrum decreases and the Li donor line increases, as one would expect. At the same time, the observed strain sensitivity of the Li line increases. Note in Fig. 6 that the Li line has essentially zero strain sensitivity. As the fluence decreases, this sensitivity increases, until at zero fluence the Li line all but disappears in the absence of externally applied stress. It is as though at high fluences, i. e., in the presence of a large number of defects, the Li is already in an appreciable strain field and does not need external stress to lift its ground-state's degeneracy. This may suggest that the

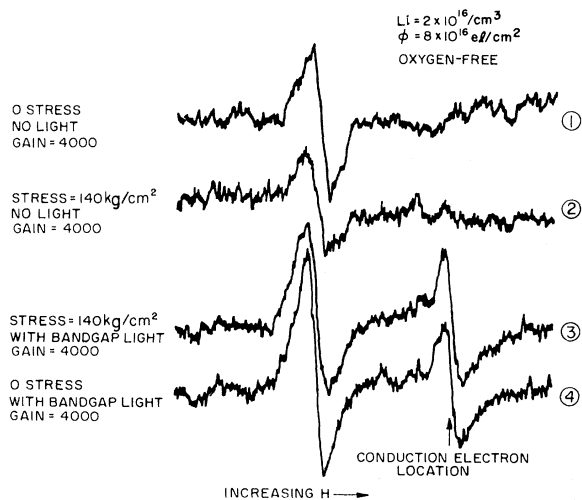


FIG. 6. EPR spectrum of electron-irradiated O-free Si. The damage line is at the left; The Li line is at the conduction electron resonance location.

reason (Li-O) has a visible EPR absorption is that the neighboring O produces a local region of strain in which the Li finds itself, which is much greater than the random strains ordinarily found in the lattice.¹⁸

After several days at room temperature, different effects take place in O-containing and O-free material. In O-containing material both the four-line damage spectrum and the (Li-O) donor line decrease sharply. Band-gap light does not restore the spectra. In O-free material, for those samples in which the carrier concentration increases (see Fig. 3) the defect spectrum disappears and the Li donor increases: In those samples where the carrier concentration decreases, however, both the Li donor EPR and the Li-defect EPR disappear.

2. Irradiation at 40 °K

The purpose here was to produce primary defects at a temperature where neither defect nor impurity was mobile, and then heat the Si to successively higher temperatures before recooling to 20 °K for the EPR measurement. In O-free material, irradiations with 1-MeV electrons at fluences up to $8.4 \times 10^{18}/\text{cm}^2$ produced no defect spectra²⁷ at temperatures up to 475 °K (the limit dictated by the indium vacuum seals, see Fig. 1). In fact, there was very little decrease in the Li donor resonance at 40 °K. Irradiation with 1.5-MeV electrons, however, did produce a sharp decrease in the intensity of the Li donor line, and beginning at about 200 °K, the onset of the Li-defect one-line spectrum shown originally in Fig. 6. Simultaneously with the growth of this line, a decrease of the Li donor line was observed. At temperatures beyond 250 °K, the Li-defect line decreases and finally disappears at about 300 °K. Above 300 °K, there is essentially no change in the defect spectra until about 475 °K where a new group of defect lines begins to emerge. However, because of the temperature limitation, these could not be studied in any detail. In Fig. 7, we have plotted the temperature behavior of the intensity of both the Li-defect and Li donor lines, where it can be seen that the decrease of the Li donor line is clearly associated with the rise of the Li-defect line.

We next irradiated at 95 °K, hoping to increase the introduction rate of the primary defect (s) which may be involved. We were unsuccessful, however, and even though strong temperature-dependent behavior for defect production has been reported for n -type material,³ we did not observe any in this experiment.

In O-containing Si we could not produce the four-line spectrum under any circumstances when we first irradiated with 1-MeV electrons at a low temperature and then heated the sample. Only by irra-

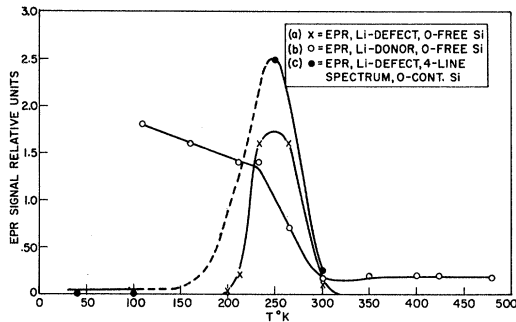


FIG. 7. Temperature dependence of Li EPR lines: (a) Li-defect line in O-free Si. $T_{\text{irr}} = 40^\circ\text{K}$. (b) Li donor line in O-free Si. $T_{\text{irr}} = 40^\circ\text{K}$. (c) Li-defect four-line spectrum in O-containing Si. For (a) and (b) the abscissa is the annealing temperature. For (c) the abscissa is the irradiation temperature. Measurement temperature is 20°K . The dashed line indicates that for this curve no data points were taken in this region.

diating at higher temperatures could this spectrum be produced. This behavior is also plotted in Fig. 7, with the important exception that for the O-containing sample the abscissa is the irradiation temperature. It may be worth noting that irradiation with fluences of $1 \times 10^{19}/\text{cm}^2$ at 40 and 100°K did not produce the four-line spectrum, while fluences of only $6 \times 10^{17}/\text{cm}^2$ and $2 \times 10^{18}/\text{cm}^2$ at 250 and 300°K , respectively, did produce it. In all cases, in O-containing Si, whatever the magnitude of the (Li-O) donor EPR, it essentially disappears at about 300°K .

III. DISCUSSION

Several properties of the radiation damage resulting from 1–1.5-MeV electron irradiation of Li-doped Si can be deduced from the experimental data presented here. The role of oxygen is clearly important. Its pairing with Li and with defects and its effect on Li diffusion are probably all involved. Depending on whether or not O is present, EPR data show that different defects form, carrier-removal data show that total defect introduction rates are different, and the low-temperature irradiation data indicate that the formation mechanism of the defect complexes is strongly affected.

The paramagnetic damage centers discussed here are comprised of Li, O and some primary defect (s) in O-containing material, and of Li and some primary defect (s) in O-free material. In addition, temperatures of about 200°K are required, suggesting that some considerable thermal energy is necessary for their formation. In their observable state, the centers are filled and have an electron spin of $\frac{1}{2}$. The energy levels are almost certainly deeper than the shallow donors. The centers which are observable by EPR are only a fraction of the total number of defects produced.

At room temperature, the EPR spectra and the carrier concentration change with time. These changes are different for O-containing and O-free material, although there is always consistency between the EPR behavior and the resistivity behavior. In the O-containing case the damage spectrum, the (Li-O) donor spectrum and the carrier concentration all decrease with time. This strongly suggests that levels, not visible by EPR, are forming. The fact that band-gap light does not restore, or even enhance, the spectra suggests that the original damage levels and donor levels (seen in Fig. 4) have disappeared (or at least been changed) rather than been merely depopulated. One likely mechanism for this is that Li diffuses and complexes with an existing defect center, even one which may already contain one Li atom. Such a mechanism is consistent with Li's mobility at room temperature, and is also in line with previous suggestions for the formation of Li-defect complexes at room temperature.⁶

In O-free material the situation appears to be more complex. Two behaviors have been observed. The first is the disappearance of the EPR damage spectrum and, simultaneously, the growth of both the donor spectrum and the carrier concentration (as in Fig. 3). This suggests an actual dissociation of the Li-defect complex, which makes more Li available to resume its role as a shallow donor. The second, observed in some samples, is the simultaneous decrease in the Li-defect EPR, the shallow donor EPR, and the carrier concentration. Here, just as the O-containing case, the evidence points to the formation of deeper defect levels which removes Li donors in the process.²⁸ Here too, the diffusion of Li may be important, and the fact that these changes take place more rapidly than analogous changes in O-containing material is consistent with the more rapid diffusion of Li in O-free material.¹⁴

Our discussion concludes with an attempt to define the paramagnetic damage centers described here and the way in which they form. It has been previously reported that phosphorus-doped³ or Li-doped⁹ *n*-type Si which contains O has a reverse annealing stage (in total carrier removal and reciprocal mobility) starting at about 200°K , i. e., a defect begins to form at this temperature and the formation does not depend on the dopant. We show this behavior in Fig. 8. We show our own data, described earlier, in Fig. 7. Examination of these two figures suggests that all these results originate from the same, or closely related, threshold process. Since at 200°K none of the impurities is mobile, we suggest that the formation of these defect complexes is due to the fact that some lattice defect has become available and sufficiently mobile to be trapped by an impurity or an impurity-involved complex.

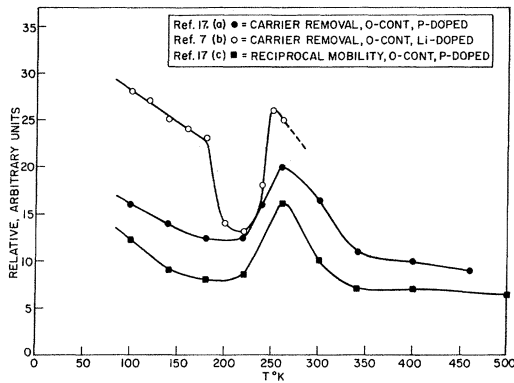


FIG. 8. Annealing curves in terms of unannealed damage versus temperature. Note that all curves show "reverse annealing," i. e., defect formation, at about 250 °K.

The identification of the defect whose availability and/or mobility allows it to be trapped is a matter of some speculation. The low-temperature electron irradiation produces primary defects, i. e., vacancies, divacancies, and interstitials. Among these the weight of existing evidence seems strongly to favor the interstitial. The divacancy itself cannot be the primary defect involved since it is known not to become mobile until about 500 °K.^{29,30} Furthermore, it should not be the vacancy, for if it were, we would expect to see the defect complex form at a much lower temperature than 200 °K: In *n*-type Si the vacancy becomes mobile at about 70–80 °K¹¹ and vacancy interactions have been observed well below 200 °K. On the other hand, some evidence does exist which suggests that in *n*-type Si the interstitial becomes mobile at temperatures of about 140–170 °K,¹¹ and that it can complex with O.³¹ These facts tend to point to the interstitial. Finally, consider that the *g* values of the EPR spectra of both Li-defect complexes are isotropic; specifically, they do not have the typical axial symmetry found for defects involving broken or dangling Si bonds (e. g. vacancies). The EPR absorption we are seeing appears to be that of a single *S*-state electron. We consider the isotropic character of the *g* values to be supportive evidence for the inter-

stitial rather than the vacancy being the primary lattice defect involved. Thus, we suggest that the defects we are seeing here are a (Li-O-interstitial) complex in O-containing material, and a (Li-interstitial) complex in O-free material.

If the interstitial can indeed complex both with O³¹ and with (Li-O), then this competition for the interstitial's capture could explain why in O-containing material only irradiation at the higher temperature (e. g., ~250 °K) enables us to observe the (Li-O-interstitial) complex. If we irradiated at lower temperatures (40 °K) the interstitial would have a chance to be preferentially trapped by O before being trapped by a (Li-O) pair. Note that in O-free material, where such competition would not be present, we can irradiate at 40 °K and still see the formation of the (Li-interstitial) complex at 200 °K.

Detailed microscopic models of the Li-defect complexes are difficult to discuss. We did not observe in our work two of the most important parameters which commonly supply information for such discussion, i. e., an anisotropic *g* value and hyperfine interaction with neighboring Si²⁹ nuclei. We do know that both Li and O are normally in interstitial positions, and a detailed model of the (Li-O) complex has been suggested.³² However, it seems fruitless to speculate on the addition of interstitial Si either to Li or to (Li-O) without any firm geometrical data, except to mention that there does seem to be ample room for these atoms in the wide <110> channel.

ACKNOWLEDGMENTS

The author is very pleased to acknowledge the timely assistance of F. Kolondra who operated the Van de Graaff accelerator. He would also like to thank G. Brucker and B. Faughnan for stimulating and helpful discussions, and N. Di Guisepe for his technical assistance. He would also like to express his deep appreciation to the members of the Groupe de Physique des Solides of the Ecole Normale Supérieure, for their professional and personal hospitality—with special words of thanks to P. Baruch, A. BreLOT, and M. Squelard for their time and helpfulness in many situations.

[†]Work partially supported by Air Force Cambridge Research Laboratories, Office of Aerospace Research, under Contract No. F19628-68-C-0133; by the Délégation Générale de la Recherche Scientifique et Technique, and by the Centre National d'Etudes Spatiales.

*Permanent address: RCA Laboratories, Princeton, N. J.

[‡]Laboratoire Associé au Centre National de la Recherche Scientifique.

¹P. Rappaport and J. Loferski, Phys. Rev. **111**, 432 (1958).

²J. W. Corbett, in *Radiation Effects in Semiconductors*,

edited by F. Vook (Plenum, New York, 1968), p. 3.

³F. L. Vook and J. L. Stein, Ref. 2, p. 99.

⁴E. L. Elkin and G. D. Watkins, Phys. Rev. **174**, 881 (1968).

⁵B. Goldstein *et al.*, Contract No. NAS 5-9131, 1966 (unpublished).

⁶J. Wysocki *et al.*, Appl. Phys. Letters **9**, 44 (1966).

⁷V. Vavilov, *Radiation Damage in Semiconductors* (Dunod, Paris, 1965).

⁸R. C. Young *et al.*, J. Appl. Phys. **40**, 271 (1969).

⁹G. Brucker, Phys. Rev. **183**, 712 (1969).

¹⁰The contributions of EPR studies to our understanding

of radiation-damage processes have been well documented: The details of the mathematical formalisms within which EPR results are generally analyzed can be found in several publications, e.g., Refs. 11 and 12.

¹¹G. Watkins, in *Effets Des Rayonnements Sur Les Semiconducteurs* (unpublished).

¹²G. Watkins, *IEEE Trans. NS-16*, No. 6 (1969).

¹³B. Goldstein, *Phys. Rev. Letters* **17**, 1 (1966).

¹⁴E. M. Pell, *Phys. Rev.* **119**, 1222 (1960).

¹⁵G. D. Watkins *et al.*, *J. Appl. Phys.* **30**, 1198 (1959).

¹⁶This step also removed the surface EPR states.

¹⁷This was "Wetalloy-232" obtained from the Victor King Laboratories.

¹⁸R. L. Aggarwall *et al.*, *Phys. Rev.* **138**, A882 (1965).

¹⁹G. D. Watkins, *Bull. Am. Phys. Soc.* **10**, 303 (1965).

²⁰G. D. Watkins and J. W. Corbett, *Phys. Rev.* **134**, A1359 (1964).

²¹J. Bourgoin *et al.*, in *Radiation Effects* (to be published).

²²The first report of such changes was made by Carter [*IEEE Trans. NS-14*, 110 (1967)] on float-zone material, although the report of spontaneous recovery of radiation-

damaged solar cells at room temperature, Ref. 9, should perhaps also be mentioned.

²³G. Feher, *Phys. Rev.* **114**, 1219 (1969).

²⁴I am indebted to G. Watkins for this information prior to publication.

²⁵The Fermi level here must be somewhere within $\lesssim kT$ (0.0023 eV) of the shallow donor energy.

²⁶G. Watkins, in *Radiation Damage in Semiconductors* (Dunod, Paris, 1965).

²⁷The over-all sensitivity of our instrumentation was such that we should have seen defect introduction rates as low as 10^{-4} cm^{-1} .

²⁸Hall measurements (of carrier concentration and mobility) have recently been made which indicate that both Li-defect formation and Li-defect dissociation can take place with time at room temperature in Li-doped electron-irradiated Si [G. Brucker (private communication)].

²⁹G. Watkins and J. Corbett, *Phys. Rev.* **138**, A543 (1965).

³⁰L. Cheng *et al.*, *Phys. Rev.* **152**, A761 (1966).

³¹R. E. Whan, *J. Appl. Phys.* **37**, 3378 (1966).

³²R. M. Chrenko *et al.*, *Phys. Rev.* **138**, A1775 (1965).

Properties of Spontaneous and Stimulated Emission in GaAs Junction Lasers. I. Densities of States in the Active Regions

C. J. Hwang

Bell Telephone Laboratories, Murray Hill, New Jersey 07974

(Received 27 March 1970)

The densities of states in the conduction and valence bands appropriate for the p region of the junction have been calculated self-consistently in the screened potential and effective-mass approximations. Such a density of states for one particular band consists of a tail part taken from the theory of Halperin and Lax, an unperturbed parabolic density of states above the tail, and a smooth interpolation in between. The use of the unperturbed parabolic band is justified, since the perturbation technique of Bonch-Bruевич and a straightforward second-order perturbation calculation both show that the distortion of the band due to the presence of impurities at the concentration employed in a typical laser is less than 5%. Contrary to the generally accepted assumption and Stern's calculation using Kane's density of states of a long and reasonable large conduction band tail, our results show that the tail is negligibly small compared to the valence band tail. On the basis of this calculation, it is concluded that, for a typical laser, the electron quasi-Fermi level at lasing threshold for temperature above 77 °K should be in the parabolic portion of the band and not in the tail as is often assumed without justification. The approximations of using linear screening for the impurity potentials and the Gaussian statistics for the impurity distribution which are implied in the density-of-state functions of Kane and of Halperin and Lax are considered in detail.

I. INTRODUCTION

Calculation of the properties of a semiconductor laser usually starts by computing the spontaneous emission rate in the region where the recombination takes place. Many of the observed characteristics of a GaAs junction laser such as the temperature dependence of the threshold current,¹⁻⁶ the lasing wavelength shift as a function of injection current,⁷ the rate,⁸ and the band shape² of the spontaneous emission have been interpreted by different

models, using various expressions for the density of states involved in the optical transitions. These calculations have been made either with or without the momentum-conservation selection rule but all have assumed a constant matrix element for the radiative transitions. In the calculations with the selection rule preserved, parabolic densities of states have been used for both the conduction and valence bands to compute the recombination rate and the stimulated emission function either on the